

## 1A.5 INFLUENCE OF EMBEDDED CONVECTION ON MICROPHYSICS OF SNOWFALL

Björn Baschek\*, Raphael Schefold, Eszter Barthazy

Institute for Atmospheric and Climate Science, ETH, Zürich, Switzerland

### ABSTRACT

The connection between embedded convection and riming is generally acknowledged. However, experimental observations of the riming degree of ice crystals together with convective parameters are scarce and several questions cannot be answered satisfactorily:

Which dynamic or thermodynamic reasons are causing embedded convection? What are suitable means for a quantification? What are the correlations to the microphysics of riming? The answers to these questions are of fundamental interest to understand the formation of precipitation and thus also of interest for, e.g., high resolution weather modelling. To answer some of the open questions, a field experiment is in progress in the pre-Alpine region of Switzerland.

The Doppler velocity, measured with a vertically pointing radar, is a combination of particle fall velocity and vertical wind speed. The vertical winds can be estimated out of combined data from radar and optical spectrometer, which is measuring size and velocity of hydrometeors.

A convective index – based on the X-band radar data – is used to quantify embedded convection in stratiform precipitation. Ice crystals are replicated (Formvar) to determine their riming degree. For case studies, a coupling between the degree of riming and convectivity is shown.

### 1. INTRODUCTION

This work is considering two different kinds of phenomena – a microphysical one (riming) and a dynamical one (embedded convection) – and their coupling.

Riming, which is the freezing of supercooled cloud droplets on snow crystals, is one of the fundamental

snow growing processes and important for, e.g., scavenging. The degree of riming – the amount of accreted supercooled cloud water on ice crystals – can be expressed on a scale of six classes (Table 1; examples Figure 1) with increasing number of frozen on cloud droplets. Embedded convective cells or "cellular overturning" (Houze and Medina, 2003) in stratiform (Houze, 1997) precipitation could be a reason for riming. The classical separation into stratiform and convective regimes of precipitation is quite rough. A more detailed classification is needed for finding a connection between embedded convection and riming and for explaining differences in the degree of riming.

Riming Degree	Description
0	unrimed
1	lightly rimed
2	moderately rimed
3	densely rimed
4	heavily rimed
5	graupel

**Tab. 1:** Classification of riming with increasing number of frozen up cloud droplets (Mosimann, 1995).

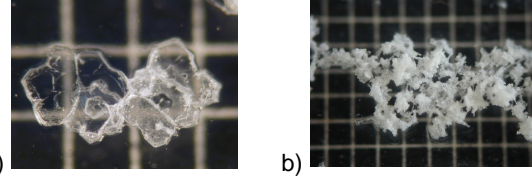


**Fig. 1:** Formvar replica of an unrimed (class 0) crystal (a) and of a densely rimed (class 3) snowflake (b). The grid size is 1 mm.

Which further split-up can be made? How well is embedded convection detectable with the help of X-band radar? Classification of convection has been made before; by, e.g., Mosimann (1995) for vertical X-band radars via the variability of the mean Doppler velocity with a convection index. A variation of this index (section 2) is used to analyze the correlation between riming and embedded convective cells in a case study (section 4).

### 2. QUANTIFICATION OF CONVECTION

$$\kappa = \frac{|v - \langle v \rangle_t|}{\langle v \rangle_t} \quad (1)$$

Equation 1 is the definition of a convection index  $\kappa$ , as introduced by Mosimann (1995). The numerator term  $|v - \langle v \rangle_t|$  is a measure of the variability of the Doppler velocity, with  $v$  being the Doppler velocity at a certain time and height and  $\langle v \rangle_t$  the average over a period of time (in our study 5 minutes) at constant height. The average velocity as denominator term  $\langle v \rangle_t$ , gives smaller absolute changes of  $\kappa$  with fluctuations for higher average velocities. With the above definition the value of  $\kappa$  is becoming negative for negative average Doppler velocities.

The equation provides a value for every height step. If wanting to follow the growth history of a snow crystal and to consider how convective its environment has been during its formation, an integration or averaging of  $\kappa$  over height is a possibility. But for this the above definition of  $\kappa$  is not suitable. First because it has a singularity for an average velocity of 0 m/s. Second because negative values of  $\kappa$ , which are describing even more convective situations, could cancel with positive values while averaging.

As a straight forward method a modified convection index  $\kappa_{mod}$  (Equation 2) has been chosen:

$$\kappa_{mod} = \begin{cases} \alpha & \kappa \geq \alpha \text{ or } \kappa \leq 0, \\ \kappa & \text{else.} \end{cases} \quad (2)$$

\*Corresponding author's address: Institute for Atmospheric and Climate Science, ETH, 8093 Zürich Switzerland; e-mail: baschek@iac.unm.ethz.ch

The original  $\kappa$  is cut at a constant value  $\alpha$  and the same value  $\alpha$  is given to negative  $\kappa$ . For a comparison with riming, convectivity is computed by averaging  $\kappa_{mod}$  over height (Equation 3;  $n$  = number of height steps) and multiplied by a second constant  $\beta$ ; with  $\alpha \cdot \beta = 5$ ,

$$\text{Convectivity} = \beta \cdot \left( \sum_{\text{height}_0}^{\text{height}_1} \kappa_{mod} \right) / n. \quad (3)$$

This gives the same value range between 0 and 5, as the riming degree. For the following case studies  $\alpha = 0.6$  and thus  $\beta = 8.3$  have been chosen.

### 3. SETUP

Mount Rigi was chosen as measuring site, having a steep rising front pointing towards the lowlands and the main weather direction. The setup, as seen in Figure 2, is split up in two locations – one at the bottom and one close to the top. The steepness of the mountain allows to measure variables on different height levels at similar horizontal position.

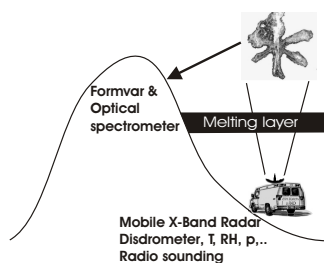


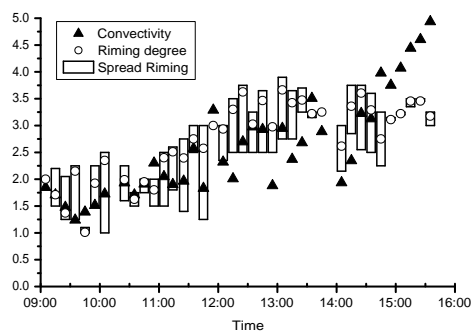
**Fig. 2:** Setup scheme with two locations, one at the bottom and the second close to the top of the mountain.

below the melting layer. It is measuring and saving the full Doppler spectrum of the precipitation particles with 0.125 m/s velocity resolution. For measuring the rain-drop size distribution, a Joss-Waldvogel-disdrometer is used. In addition, standard meteorological parameters are monitored and radio soundings can be performed. Close to the top of the mountain (1600 m above sea level, 1150 m above the radar), snowfall is observed with an optical spectrometer (see Schefold et al. (2002) for more details), measuring shapes and the size distribution of the ice particles and their fall velocities, which are influenced by the degree of riming. In addition, ice crystals are replicated with the Formvar method to determine their size, type and riming degree. Radio soundings are performed and the wind field around the experimental site is monitored with one resp. two C-band Doppler radars, working in single- resp. dual-Doppler mode.

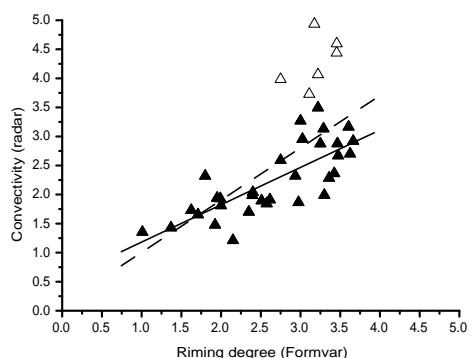
### 4. CASE STUDY

From the cases studies, which have been taking place in the winter season 2002/2003, as a first example 7 November 2002 has been chosen. Precipitation was caused by an occlusion. In the chosen 7 hour period, the rain rates were relatively low (per minute rain rate up to 7.3 mm/h, with 0.7 mm/h average

and 4.7 mm in total). Temperature at the bottom station rose from 4.1° to 6.2° C, falling again for the last half hour. At the top station, the temperature ranged between -1.5° and -2° C. Figure 4 shows the height-time-indicator (HTI) of reflectivity (a) and of the Doppler velocity (b) for this period. A bright band with varying strength and an increasing number and size of areas with close to zero or negative Doppler velocities – a clear indication of embedded convective cells – can be seen. The increase in cellular structure can even be seen in the reflectivity HTI.



a)



b)

**Fig. 3:** Change in riming degree and convectivity versus time (a) and scatter plot of convectivity versus riming degree (b). The data points of the last one and a half hours are marked with the empty triangles. The straight lines are fits with (dashed) and without (solid) these last data points.

The modified convection index has been computed, applying equation 3, and averaged over the height range 2 km above the height level of the top station. The result is shown in Figure 3a together with riming. The degree of riming is estimated from analysis of the Formvar samples, taken at the top station. At the beginning of the period, the degree of riming has been about 1.5, started then to rise and had at the end of the period a degree of about 3.5. For computing the correlation between riming degree and convectivity, the convectivity has been averaged over the 10 minute periods around the Formvar sampling times (38 in total). A scatter diagram of convectivity versus riming degree is shown in Figure 3b. The computed correlation is 0.67 resp. 0.77 if skipping the last one and a half hours (marked with empty triangles), which had stronger convection.

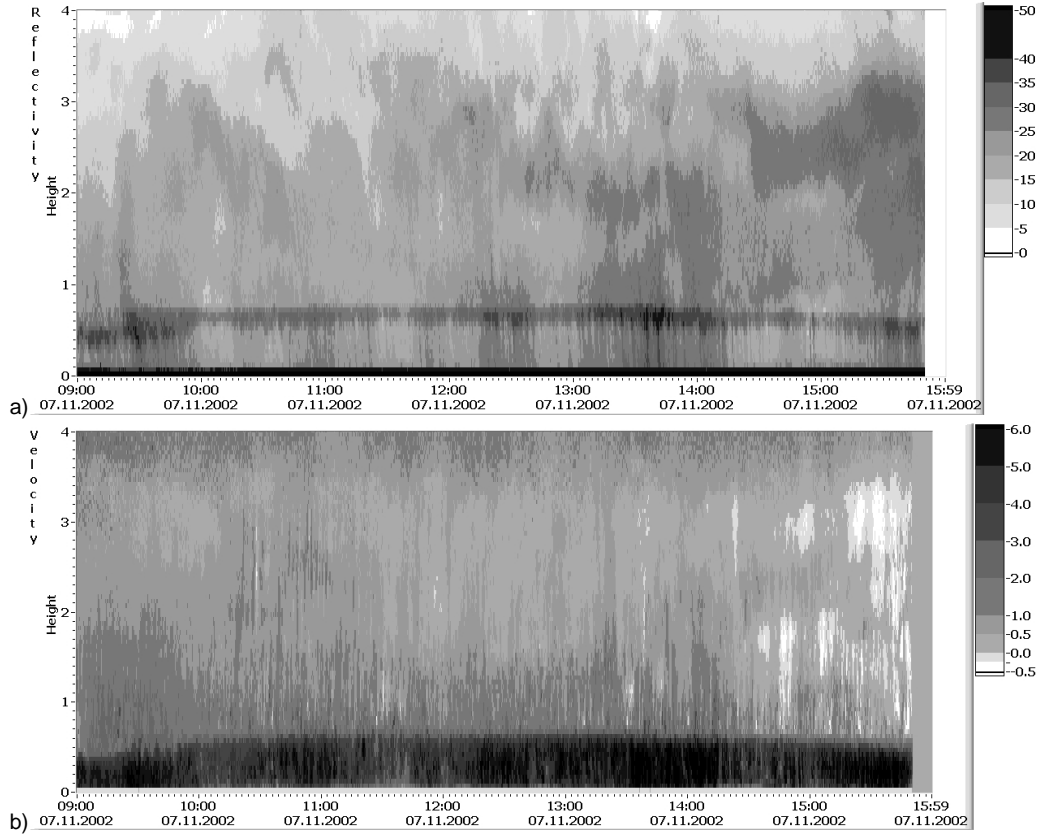


**Fig. 4:** Height time diagram (HTI) of reflectivity (a) and Doppler velocity for a 7 hour period on 7 November 2002. An increasing number of embedded convective cells can be seen. (In color at: <http://www.iac.ethz.ch/staff/bjoern/>.)

## 5. DISCUSSION OF THE CASE STUDY

The correlation between riming and convectivity, deduced from the straight forward modification of the convection index, is astonishing high. If the updraft regions are large – as in the last one and a half hours of our case – an increase of convectivity with higher riming can be seen, which is stronger than the slope of the linear fit. This can possibly be explained by the non-linearity of the riming scale. The increase in rimed mass per riming degree is much smaller for low than for high riming degrees. Besides, the modified convection index seems to be overestimating the influence of updrafts. It might be possible to separate their influence (section 7). This might give clues to the understanding of different influencing aspects of convectivity and effects by larger scale vertical winds to riming, such as relative velocities, condensation and prolonged residence time in the clouds.

Equation 4 (Klett and Pruppacher (1997)) is describing the increase in mass of a raindrop (mass  $m_1$ , radius  $a_1$ ) by collecting smaller raindrops (radius  $a_2$ ) with a collection kernel  $E_c$ :

$$\frac{dm_1}{dt} = \frac{4\pi\rho_w}{3} \int E_c \cdot \pi(a_1 + a_2)^2 \cdot (v_{\infty,1} - v_{\infty,2}) \cdot a_2^3 n(a_2) da_2. \quad (4)$$

Applying this standard collection equation to riming, it can give us some ideas, what is happening during

riming, taking the large collecting raindrop for the ice crystal and the collected smaller raindrops for the supercooled cloud droplets. Besides convectivity and vertical winds, there might be other influencing factors, e.g., concentration, size and habit of ice crystals, and size distribution of cloud droplets ( $a_2^3 n(a_2) da_2$ ), and wind speed and turbulence, influencing the relative velocities ( $v_{\infty,1} - v_{\infty,2}$ ).

## 6. EXTENSION TO OTHER CASES

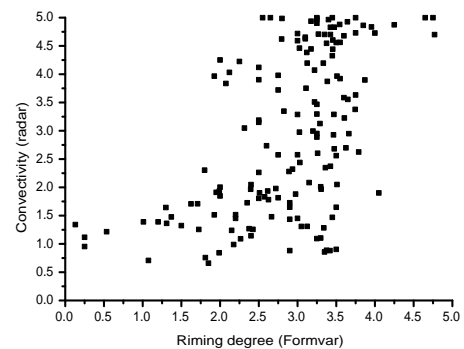


**Fig. 5:** Scatter plot of convectivity versus riming degree for all 9 cases of winter 02/03.

Figure 5 shows a first sketch of a scatter plot of convectivity versus riming for all 9 cases of winter 02/03 (159 Formvar samples; temperature  $< -1^{\circ}\text{C}$ ). Also here, an increase of convectivity with higher riming can be seen, which is stronger than the one of the linear fit in the above case study. The strong scatter in this plot can probably be minimized by closer analysis, if, e.g., considering a possible time lag between measurements at top and bottom station and adapting averaging range individually to the cases.

## 7. VERTICAL WINDS

A method to estimate the strength of vertical winds is being developed. For this, a combination of optical snow spectrograph (disdrometers could be used in a similar way in rain) and radar data is used.

The radar is measuring the reflectivity and the Doppler spectrum in "free air". The Doppler velocity  $v_D$  is defined as the first moment of the velocity distribution:

$$v_D = \frac{\int_{-\infty}^{+\infty} z_v \cdot v \cdot dv}{z} . \quad (5)$$

For a vertically pointing radar, the velocity  $v$  is the sum of the "intrinsic" fall velocity of the particles and the vertical wind speed  $w$  (updrafts negative sign;  $v$ ,  $v_0$  positive for falling particles), if assuming, that all particles are equally influenced by the vertical wind:

$$v = v_0 + w . \quad (6)$$

The optical spectrometer is measuring size distribution and velocity of hydrometeors at the ground. With the boundary condition, that vertical winds are zero ( $w = 0$ ) at the ground, the measured velocity is equal to the intrinsic fall velocity:  $v = v_0$ .

The particles measured by the optical spectrometer can be split into velocity bins. If the radar reflectivity is computed separately for these bins, a Doppler spectrum is achieved. A simple approach for the computation of the reflectivity is via the "reflectivity factor"  $\Sigma D^6$ , with consideration of the smaller dielectric factor for ice spheres. This is a good approximation for solid ice. For aggregates one had to correct for the low density. Because of this, some authors propose an approach proportional to the the fourth power of the diameter (Hogan et al., 2002).

Of course, the circumstances are getting even more complicated for larger particles, if the Rayleigh scattering regime is left.

An advantage is, that for the computation of the Doppler velocity via the first moment of the received distribution, not the scaling, but only the shape of the Doppler spectrum is important. Furthermore, by comparison of the zeroth moment of the Doppler spectrum received from the snow spectrograph with the reflectivity measured by the radar, a test of the assumptions during the calculation can be performed.

Finally, the vertical wind speed for one height can be estimated, by subtracting the Doppler velocity, computed from the snow spectrograph data, from the Doppler velocity, measured by the radar at the equivalent height of the mountain station:

$$w = v_{D,\text{radar}} - v_{D,\text{spectrometer}} . \quad (7)$$

Thus, a separation of the influence of continuous updrafts from the influence of convection on riming

could be possible for this height level. Problematic situations with strong vertical wind shear might be recognizable by comparing the computed with the measured Doppler spectra.

## 8. CONCLUSIONS & OUTLOOK

For a case study, a correlation could be found between the degree of riming and convectivity, caused by embedded convective cells. They can be seen in the reflectivity and Doppler data of the X-band radar – quantified by a convection index. A first application to other case studies shows a similar connection, but with a stronger rise of convectivity for higher riming degrees. This might be due to the non-linear character of the riming scale or a too strong weight for negative average velocities in the modified convection index. Fits might be optimized by filtering the data, considering time shifts between measurements or using other convection indices. Further analysis will have to be done carefully. Meteorological conditions and other microphysical aspects have to be considered and the influence of vertical winds could be separated with the help of the above described method.

Further plans are e.g. to identify with help of the dual Doppler wind fields special synoptic and orographic situations, which are the reason for the generation of embedded convective cells in stratiform winter precipitation and thus creating prerequisites for riming to occur.

## ACKNOWLEDGMENTS

The authors wish to express their appreciation to Markus Stucki for his help with the field campaigns.

## References

- Hogan, R. J., Field, P. R., Illingworth, A. J., Cotton, R. J., and Choulaton, T. W. (2002). Properties of embedded convection in warm-frontal mixed-phase cloud from aircraft and polarimetric radar. *Quarterly Journal of the Royal Meteorological Society*, 128(580):451.
- Houze, R. A. (1997). Stratiform precipitation in regions of convection: A meteorological paradox? *Bulletin of the American Meteorological Society*, 78(10):2179.
- Houze, R. A. and Medina, S. (2003). Orographic enhancement of precipitation in midlatitudes: Results from map and improve ii. In *Preprints, ICAM/MAF 2003, Brig, Switzerland*, pages 1–3.
- Klett, J. D. and Pruppacher, H. R. (1997). *Microphysics of clouds and precipitation*. Kluwer Academic Publishers, Dordrecht [etc.], 2nd edition.
- Mosimann, L. (1995). An improved method for determining the degree of snow crystal riming by vertical doppler radar. *Atmospheric Research*, 37(4):305.
- Schefold, R., Baschek, B., Wüest, M., and Barthazy, E. (2002). Fall velocity and axial ratio of snowflakes. In *Proceedings of ERAD (2002)*, page 84.

More information: <http://www.iac.ethz.ch/staff/bjoern>.